JOC Article

Stereodynamics and Conformational Chirality of the Atropisomers of Ditolyl Anthrones and Anthraquinone

Lodovico Lunazzi, Michele Mancinelli,† and Andrea Mazzanti*

Department of Organic Chemistry "A. Mangini", University of Bologna, Viale Risorgimento 4, Bologna 40136, Italy

mazzand@ms.fci.unibo.it

Received March 26, 2008

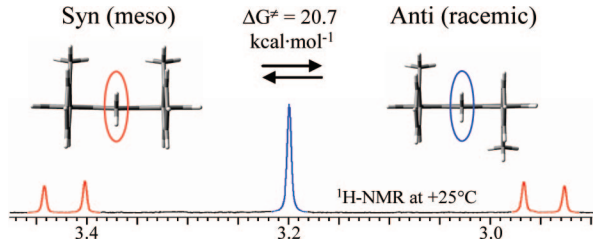

Syn and anti conformers in similar proportions were observed at ambient temperature for the title compounds. The conformational assignment of the two anthrones was obtained by the observation of different multiplicity of the methylene NMR signals, whereas that of the anthraquinone derivative was determined by NOE experiments. The anti-to-syn interconversion barriers were obtained by line-shape simulation of the temperature-dependent NMR spectra, and by saturation tranfer experiments. In one case the X-ray diffraction indicated that the syn is the only structure observed in the crystals.

Introduction

It has been recognized that π-stacking interactions of aromatic substituents bonded in appropriate positions to planar (or quasiplanar) frameworks[1] play an important role in a great number of chemical properties, including stereocontrolled reactions,[2] molecular recognitions,[3] nucleic acid and protein structures,[4] and crystal packing.[5] Depending on the hindrance of the aryl substituentes and on the type of the planar framework (e.g., benzene,[6] naphthalene,[7] phenanthrene, [8] anthracene,[9] acenaphthene,[10] and acenaphthalene[11]), the resulting atropisomers can be either stereolabile or configurationally stable. This type of atropisomer should be also observable when anthrone or antraquinone are used as a framework to which connect the appropriate aryl substituents. The interest for synthesizing and studying these derivatives is due to the fact that they can be further functionalized quite easily, owing to the presence of the carbonyl moiety, whereas the compounds investigated so far, being hydrocarbons,[6–11] are less prone to undergo further modifications. In the present work we report the experimental detection of atropisomers occurring in the isomeric 1,9-ditolylanthrones and anthraquinone (**1**−**3** in Chart 1), as well as the determination of the barrier required for their interconversion.

† In partial fulfilment of the requirements for the Ph.D. degree in Chemical Sciences, University of Bologna.

(1) Cozzi, F.; Annunziata, R.; Benaglia, M.; Cinquini, M.; Raimondi, L.; Baldridge, K. K.; Siegel, J. S. *Org. Biomol. Chem.* **2003**, *1*, 157–162.

(2) Jones, G. B. *Tetrahedron* **2001**, *57*, 7999–8016.

(3) (a) Diederich, F. *Angew. Chem., Int. Ed. Engl.* **1988**, *27*, 362–386. (b) Smithrud, D. B.; Wyman, T. B.; Diederich, F. *J. Am. Chem. Soc.* **1991**, *113*, 5420–5426. (c) Conn, M. M.; Deslongchamps, G.; de Mendoza, J.; Rebek, J. *J. Am. Chem. Soc.* **1993**, *115*, 3458–3557. (d) Philip, D.; Stoddardt., J. F. *Angew. Chem., Int. Ed. Engl.* **1996**, *35*, 1154–1196. (e) Muehldorf, A. V.; Van Egen, D.; Warner, J. C.; Hamilton, A. D. *J. Am. Chem. Soc.* **1988**, *110*, 6561–6562. (f) Zimmermann, S. C.; Zeng, Z.; Wu, W.; Reichert, D. E. *J. Am. Chem. Soc.* **1991**, *113*, 183–196. (g) Newcomb, L. T.; Gellman, S. H. *J. Am. Chem. Soc.* **1994**, *116*, 4993–4994. (h) Cochran, J. E.; Parrott, T. J.; Whitlock, B. J.; Whitlock, H. W. *J. Am. Chem. Soc.* **1992**, *114*, 2269–2270.

(4) (a) Saenger, W. *Principles of Nucleic Acid Structures*; Springer Verlag: New York, 1984. (b) Burley, S. K.; Petsko, G. A. *Science* **1985**, *229*, 23–28. (c) Hunter, C. A.; Singh, J.; Thornton, J. M. *J. Mol. Biol.* **1991**, *218*, 837–846. (d) Hunter, C. A. *J. Mol. Biol.* **1993**, *230*, 1025–1054. (e) Schall, O. F.; Gokel, G. W. *J. Org. Chem.* **1996**, *61*, 1149–1458. (f) Guckian, K. M.; Schweitzer, B. A.; Ren, R. X. F.; Sheils, C. J.; Paris, P. L.; Tanmasseri, D. C.; Kool, E. T. *J. Am. Chem. Soc.* **1996**, *118*, 8182–8183. (g) Ho, T. L.; Liao, P. Y.; Wang, K. T. *J. Chem. Soc., Chem. Commun.* **1995**, 2437–2438. (h) Ranganathan, D.; Haridas, V.; Gilardi, R.; Karle, J. L. *J. Am. Chem. Soc.* **1998**, *120*, 10793–10800. (i) Chelli, F.; Gervasio, F. L.; Procacci, P.; Schettino, V. *J. Am. Chem. Soc.* **2002**, *124*, 6133–6143. (j) Chelli, F.; Gervasio, F. L.; Procacci, P.; Schettino, V. *Proteins* **2002**, *48*, 117–125.

(5) (a) Dahl, T. *Acta Chem. Scand.* **1994**, *48*, 95–106. (b) Williams, J. H. *Acc. Chem. Res.* **1993**, *26*, 593–598. (c) Anderson, H. L.; Bashall, A.; Henrick, K.; McPartlin, M.; Sanders, J. K. M. *Angew. Chem., Int. Ed. Engl.* **1994**, *33*, 429–431. (d) Dance, I.; Scuddar, M. *Chem. Eur. J.* **1996**, *2*, 481–486. (e) Wang, Z. H.; Hirose, T.; Hiratani, K.; Yang, Y.; Kasuga, K. *Chem. Lett.* **1996**, 603–604. (f) Martin, C. B.; Patrick, B. O.; Cammers-Goodwin, A. *J. Org. Chem.* **1999**, *64*, 7568–7578. (g) Nakamura, Y.; Suzuki, H.; Hayashida, Y.; Kudo, T.; Nishimura, J. *Liebigs Ann./Recl.* **1997**, 1769–1776.

10.1021/jo800677n CCC: $40.75
Published on Web 06/21/2008

CHART 1

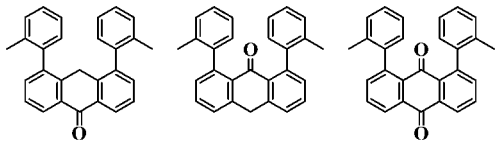

1 **2** **3**

SCHEME 1. DFT Computed Structures[a] of the Two Conformers of 1 (top) and Experimental X-ray Structure (bottom)

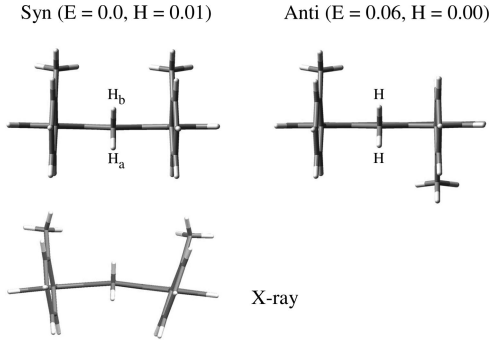

[a] The relative energies (E) and enthalpies (H) are in kcal mol^{-1}.

DFT computations predict for each compound the existence of two energy minima, corresponding to the syn and anti atropisomers generated by the restricted sp^2-sp^2 rotation. As an example, the syn and anti forms computed (at the B3LYP/6-31G(d) level) for compound **1** are displayed in Scheme 1: they are predicted to have essentially the same energy. From this picture it is evident that the two methylene hydrogens of the anti conformer experience the same environment, being related by the 2-fold symmetry axis of the molecule (C_2 point group), whereas the two methylene hydrogens (labeled H_a and H_b) of the syn conformer (C_s point group) experience different environments, and are therefore diastereotopic.[12]

Results and Discussion

The ^{1}H NMR signal of the CH_2 hydrogens of **1** (upper trace of Figure 1) displays, in fact, the four lines of an AB-type spectrum ($J_{gem} = -24.0$ Hz) along with a single line, due to the chiroptic methylene of the syn and to the achiroptical methylene of the anti conformer, in a 50:50 ratio, respectively. An analogous spectrum is also observed for the CH_2 hydrogens of **2** (i.e., a single line and an AB-type spectrum with $J_{gem} = -20.7$ Hz, as in Figure S-1 of the Supporting Information).

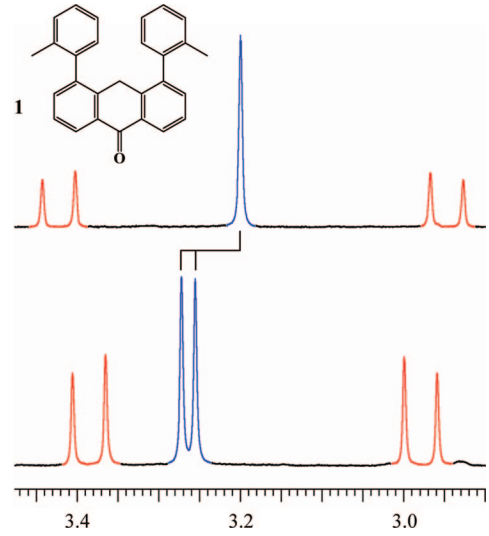

FIGURE 1. (Top) ^{1}H methylene spectrum (600 MHz in CD_2Cl_2 at −40 °C) of **1**. (Bottom) In a chiral environment the splitting of the single line (blue) of the anti (chiral) conformer but not of the four line spectrum (red) of the syn (achiral) conformer is observed.

In the case of compound **1** we could also obtain the X-ray structure (Scheme 1), which shows that solely the syn form is populated in the solid state.[13] From Scheme 1 it is evident that the central ring of anthrone is bent in the crystalline structure, while is planar in both the anti and syn calculated structures. This finding is apparently anomalous, because in the cases of **2** and **3** the DFT calculations indicate that the corresponding ground states have the central ring bent (see Figure S-2 of the Supporting Information). To check whether the discrepancy depends upon the inadequacy of the theoretical approach, calculations at higher levels (PBE1PBE/6-31+G(d,p), HF/6-31+G(d,p), and B3LYP/6-31++G(d,p)) were carried out on the **1**-*syn* conformation: in all cases, however, the central ring results invariably planar.

Two experimental observations in solution actually support the theoretical prediction of a planar structure of the anthrone ring in **1**:

(i) The large geminal coupling has been reported[14] to be a function of the dihedral angle ϕ, defined as the angle between the π orbital and an imaginary line passing through both protons of the methylene group. In the case of the calculated planar structure of **1**-*syn*, this dihedral angle is exactly 0°, thus this coupling reaches its maximum value.[14] In the case of **2**, the bent geometry of the central ring causes the dihedral angle ϕ to become about 23° (according to DFT calculations), thus reducing the value of the *J*-coupling, as experimentally observed (i.e., −20.7 and −24.0 Hz in **2** and **1**, respectively).[15]

(ii) In the case of **2**, the low-field hydrogen signal of the AB-system displays a small additional ^4J coupling (0.95 Hz) with

(6) (a) Mitchell, R. H.; Yan, J. S. H. *Can. J. Chem.* **1980**, *58*, 2584–2587. (b) Lunazzi, L.; Mazzanti, A.; Minzoni, M.; Anderson, J. E. *Org. Lett.* **2005**, *7*, 1291–1294. (c) Mazzanti, A.; Lunazzi, L.; Minzoni, M.; Anderson, J. E. *J. Org. Chem.* **2006**, *71*, 5474–5481.

(7) (a) Clough, R. L.; Roberts, J. D. *J. Am. Chem. Soc.* **1976**, *98*, 1018–1020. (b) Cozzi, F.; Cinquini, M.; Annunziata, R.; Siegel, J. S. *J. Am. Chem. Soc.* **1993**, *115*, 5330–5331. (c) Cozzi, F.; Ponzini, F.; Annunziata, R.; Cinquini, M.; Siegel, J. S. *Angew. Chem., Int. Ed. Engl.* **1995**, *34*, 1019–1020. (d) Zoltewicz, J. A.; Maier, N. M.; Fabian, W. M. F. *Tetrahedron* **1996**, *52*, 8703–8706. (e) Zoltewicz, J. A.; Maier, N. M.; Fabian, W. M. F. *J. Org. Chem.* **1996**, *61*, 7018–7021. (f) Thirsk, C.; Hawkes, G. E.; Kroemer, R. T.; Liedl, K. R.; Loerting, T.; Nasser, R.; Pritchard, R. G.; Steele, M.; Warren, J. E.; Whiting, A. *J. Chem. Soc., Perkin Trans. 2* **2002**, 1510–1519. (g) Tumambac, G. E.; Wolf, C. *J. Org. Chem.* **2005**, *70*, 2930–2938.

(8) Lai, J.-H. *J. Chem. Soc., Perkin Trans. 2* **1986**, 1667–1670.

(9) (a) House, H.; Hrabie, J. A.; Van Derveer, D. *J. Org. Chem.* **1986**, *51*, 920–929. (b) House, H.; Holt, J. T.; Van Derveer, D. *J. Org. Chem.* **1993**, *58*, 7516–7523.

(10) Cross, W.; Hawkes, G. E.; Kroemer, R. T.; Liedl, K. R.; Loerting, T.; Nasser, R.; Pritchard, R. G.; Steele, M.; Watkinson, M.; Whiting, A. *J. Chem. Soc., Perkin Trans. 2* **2001**, 459–467.

(11) Lai, Y.-H.; Chen, P. *J. Chem. Soc., Perkin Trans. 2* **1989**, 1665–1670.

(12) An opposite situation was reported in the case of the 2,6-diarylbenzoic acids (aryl being 2-methylnaphthalene), which is chiral in the anti but achiral in the syn configuration. The NMR showed, in fact, that the methylene hydrogens of the corresponding propargyl esters are diastereotopic in the anti but enantiotopic in the syn isomers. See: Chen, C-T; Chadah, R.; Siegel, J. S.; Hardcastle, K. *Tetrahedron Lett.* **1995**, *36*, 8403–8406.

(13) In the analogous case of the 1,8-di(*o*-tolyl)biphenylene, the syn structure has been also found to be the preferred form in the crystalline state; see: Lunazzi, L.; Mancinelli, M.; Mazzanti, A. *J. Org. Chem.* **2008**, *73*, 2198–2205.

(14) Renaud, R. N.; Bovenkamp, J. W.; Fraser, R. R.; Capoor, R. *Can. J. Chem.* **1977**, *55*, 2642–2648, and references cited therein.

the two hydrogens in positions 4 and 5 of the anthrone ring, whereas the high-field hydrogen signal does not display such a coupling (Figure S-1 of the Supporting Information). This implies that in compound **2**, H_a and H_b have different dihedral angles with the two ortho hydrogens, therefore confirming the bent geometry of the anthrone ring. These considerations are further supported by the DFT-calculated *J*-couplings (including the Fermi contact term) for the two syn conformers of **1** and **2**: in the case of planar **1**, in fact, the calculated J_{gem} for the syn conformer is actually predicted to be larger than that of **2** (−28.5 and −22.5 Hz, respectively). In addition, these calculations predict that H_b of compound **2** (computed to have the lower field signal) is coupled with the hydrogens in positions 4 and 5 of anthrone ($^4J = -1.34$ Hz), in agreement with the experimental 0.95 Hz value. On the other hand, H_a is predicted to have a negligible ^4J coupling (−0.02 Hz), as experimentally observed.

The presence of two enantiomers in the anti form can be demonstrated by the NMR spectrum taken in a chiral environment. In these conditions,[16] for instance, the single signal of the CH_2 moiety of **1** splits into a pair of lines due to the M,M and P,P enantiomers,[17] whereas the CH_2 signals of the achiral syn conformer are not further split (Figure 1, bottom trace): these methylene hydrogens, in fact, are already diastereotopic in the achiral solvent.

The same behavior is also observed in the corresponding ^{13}C spectrum of the two CH_2 lines: the signal at higher field splits, in fact, into a pair of lines, due to the M,M and P,P enantiomers, whereas that at lower field does not (Figure S-3 of the Supporting Information). This allows one to assign the upfield line to the anti (chiral) and the downfield line to the syn (achiral) conformer.

In the spectrum of compound **2** (bottom trace of Figure 2) the intensity of the single line of the anti is slightly higher than the intensity of the four-line spectrum of the syn (ratio 53:47). This result, apparently, is not matched by DFT computations that predict an energy lower (ΔE and $\Delta H^0 = 0.37$ and 0.40 kcal mol^{-1}, respectively)[18] for the syn with respect to the anti (Figure S-2 of the Supporting Information). It has to be taken into account, however, that the anti form is favored (by RT ln 2) by the entropy of mixing, since the anti comprises two enantiomers whereas the syn does not.[19] Accordingly, the relative computed enthalpy of the anti has to be corrected, at ambient temperature, by an entropic factor of RT ln 2 = 0.41 kcal mol^{-1} with respect to the syn. When this effect is taken into account, the anti is expected to have essentially the same

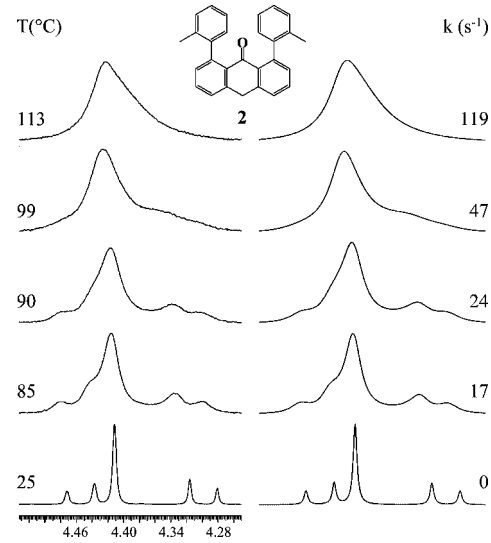

FIGURE 2. Temperature dependence of the ^1H NMR methylene signal (600 MHz in $CDCl_2-CDCl_2$) of **2** (left). On the right the simulation with the rate constants indicated (see Figure S-4 of the Supporting Information for the details of the exchange matrix).

population as the syn (in fact ΔG^0 is 0.40 − 0.41 = −0.01 kcal mol^{-1}), therefore accounting for the nearly equal population experimentally observed (if the experimental errors are considered, the 53:47 ratio does not differ significantly from 50:50). It should also be outlined that the syn has a C_s and the anti a static C_1 symmetry (assuming it has a bent geometry), and as a consequence, both have an equal symmetry number ($\sigma = 1$),[19] causing this contribution to the entropic factor to be the same, thus irrelevant.[20]

On raising the temperature, the CH_2 signals of **2** display a line-broadening effect due to the exchange of the syn and anti conformers (Figure 2): eventually these signals merge into a single line when the interconversion process becomes fast (above +110 °C). This exchange process also can be followed by monitoring the temperature dependence of the two single lines of the methyl groups (Figure 3), where the more intense line of the anti (53%) is at higher field[21] than that of the syn conformer (47%).

From the rate constants used to simulate the exchange process of the methyl lines (Figure 3), a $\Delta G^{\ddagger}$ value of 18.6 kcal mol^{-1} is obtained.[22] This barrier corresponds to the interconversion of the anti into the syn conformer that, however, can take place via a rotation of either of the two tolyl rings. To obtain the barrier corresponding to the rotation of a single tolyl ring, the values of the rate constants reported should be divided by two:[23] the corresponding barrier is, accordingly, 0.5 kcal mol^{-1} higher ($\Delta G^{\ddagger} = 19.1$ kcal mol^{-1} as in Table 1).

Since the exchange of methylene hydrogens corresponds to two subsequent single rotations of the tolyl rings, this explains why the rate constants, introduced in the matrix for simulating the spectrum of Figure 2, are one-half those of Figure 3 at the

(15) The observed difference between these two J_{gem}-couplings (24.0−20.7 = 3.3 Hz for $\phi = 0°$ and 23°, respectively) is consistent with the differences reported in ref 14 (e.g., 23.6−18.1 = 5.5 Hz for $\phi = 0°$ and 45°, respectively).

(16) Use was made of a 10:1 molar excess of enantiopure *R*-(−)-2,2,2-trifluoro-1-(9-anthryl)ethanol: Pirkle, W. H.; Sikkenga, D. L.; Pavlin, M. S. *J. Org. Chem.* **1977**, *42*, 384–387. The temperature of −40 °C was used to increase the separation of the lines (10 Hz at 600 MHz)

(17) Each of the two (blue) lines in the bottom trace of Figure 1 corresponds to the two identical (isochronous) methylene hydrogens within each enantiomer of the anti conformer. If the two hydrogens had been anisochronous, an AB-type spectrum, with a geminal *J* coupling, would have been observed; see: Fraser, R. R.; Pettit, M. A.; Miskow, M. *J. Am. Chem. Soc.* **1972**, *94*, 3253–3254. Kainosho, M.; Ajisaka, K.; Pirkle, W. H.; Beare, S. D. *J. Am. Chem. Soc.* **1972**, *94*, 5924–5926. This issue has to be addressed in that two enantiotopic groups of an achiral molecule also split their signal in a chiral environment; see: Casarini, D.; Davalli, S.; Lunazzi, L.; Macciantelli, D. *J. Org. Chem.* **1989**, *54*, 4616–4619. Casarini, D.; Lunazzi, L.; Verbeek, R *Tetrahedron* **1996**, *52*, 2471–2480. Casarini, D.; Lunazzi, L.; Mazzanti, A. *Angew. Chem., Int. Ed.* **2001**, *40*, 2536–2539. In compound **1**, in fact, not only the methyl signal of the anti but also the methyl signal of the syn conformer splits in this experiment, because the methyl groups of the latter are enantiotopic in the achiral environment, contrary to the corresponding CH_2 hydrogens that are already diastereotopic (see Figure 2)

(18) The ratio of the conformers actually depends upon the free energy $\Delta G° = \Delta H° - T\Delta S°$. DFT computations yield acceptable values for the enthalpy, but they are known to produce unreliable values for the entropy factor when low-frequency normal modes (< 900 cm^{-1}) are taken into account, as happens in the present cases; see, for instance: Ayala, P. Y.; Schlegel, H. B. *J. Chem. Phys.* **1998**, *108*, 23142325. For this reason we preferred to estimate the entropy contribution on the basis of the molecular symmetry, according to ref 19.

(19) Eliel. E. L.; Wilen, S. H. *Stereochemistry of Organic Compounds*; Wiley: New York, 1994; pp 97. and 601. See also: Lunazzi, L.; Mazzanti, A.; Minzoni, M. *J. Org. Chem.* **2005**, *70*, 10062–10066.

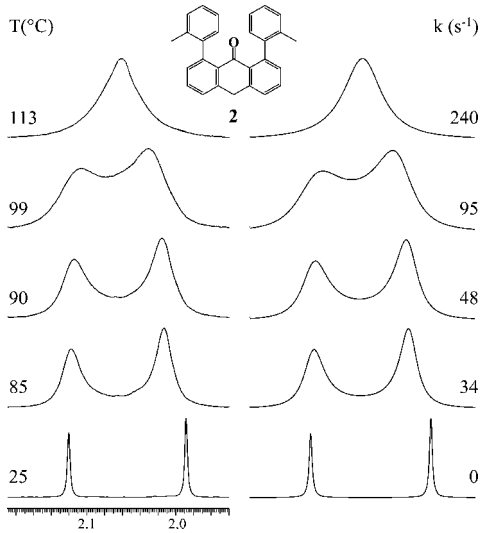

FIGURE 3. Temperature dependence of the CH_3 signals (600 MHz in $CDCl_2-CDCl_2$) of **2** (left). On the right is the spectral simulation with the rate constants indicated.

TABLE 1. Conformer Ratio and Anti-to-Syn Interconversion Barrier (in kcal mol^{-1}) [a] for Compounds 1−3

compd	1	2	3
anti:syn ratio	50:50	53:47	57:43
anti-to-syn barrier[a]	20.7 (21.2) 20.3[b] (20.8)	18.6 (19.1)	18.7 (19.2)

[a] The values in parentheses refer to the rotation barrier of a single tolyl ring (see text). [b] Data obtained from 1D-EXSY experiments.

same temperature. In the case of **1**, where the methyl signals are accidentally coincident, the corresponding anti-to-syn interconversion barrier could be obtained, by dynamic NMR approach, only by monitoring the methylene signals (Figure S-5 of the Supporting Information).

The direct anti-to-syn interconversion also can be obtained by means of an independent method, based upon the use of the saturation transfer approach (1-D EXSY as in the Experimental Section), which allows one to perform experiments at lower temperatures and to achieve rate constants much smaller than those obtainable by the DNMR method. This was accomplished by saturating the single CH_2 line of the anti conformer whereas observing the increase of the CH_2 lines of the syn conformer. In this way (see as an example Figure 4 and the Supporting Information) rate constants of 0.30, 0.44, 0.64, and 0.92 s^{-1} (at +59, +63, +67, and +72 °C, respectively) were determined

(20) When the same argument is applied to the case of compound **1**, the anti conformer should be likewise expected to be more populated than the syn, but in this case the anti has a C_2 symmetry, whereas the syn has C_s symmetry. As a consequence, the former is favored by the entropy of mixing, but it is disfavored by RT ln 2 because of the different symmetry number ($\sigma = 1$ for C_s and $\sigma = 2$ for C_2): the two entropic effects act in opposite directions and therefore cancel out. The enthalpy difference, accordingly, remains the same as that (−0.01 kcal mol^{-1}) computed in Scheme 1 and such a negligible difference accounts for the equal population experimentally observed.

(21) The methyl line of the anti is at higher field than that of the syn because it lies above the plane of the other aromatic ring, thus experiencing the well-known effect of the aromatic ring currents. See, for instance: Jackman, L. M.; Sternhell, S. *Applications of NMR Spectroscopy in Organic Chemistry*, 2nd ed.; Pergamon Press: Oxford, UK, 1969; p 95. Jennings, W. B.; Farrell, B. M.; Malone, J. F. *Acc. Chem. Res.* **2001**, *34*, 885–894. Wüthrich, K. *Angew. Chem., Int. Ed.* **2003**, *42*, 3340–3363.

(22) As often observed in conformational processes, the free energy of activation was found independent of temperature within the errors, indicating a negligible value of $\Delta S^{\ddagger}$. See: Lunazzi, L.; Mancinelli, M.; Mazzanti, A. *J. Org. Chem.* **2007**, *72*, 5391, and references cited therein.

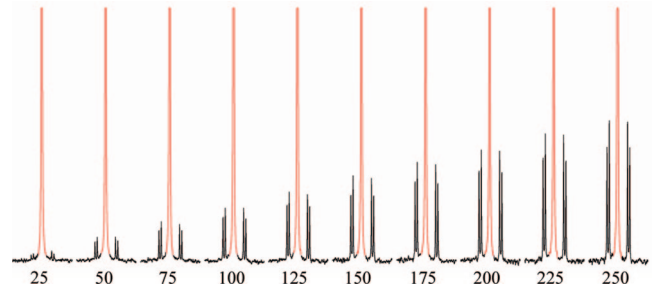

FIGURE 4. Saturation transfer experiment (1D-EXSY) for compound **1** at +72 °C (600 MHz in $CDCl_2-CDCl_2$). The AB-type CH_2 spectrum (black trace) of the syn conformer grows when raising the mixing time (in ms), after saturation of the CH_2 anti single line (red signal).

for the anti-to-syn interconversion, corresponding to a $\Delta G^{\ddagger}$ value of 20.3 ± 0.2 kcal mol^{-1}. Within the experimental error, this value agrees with that obtained by the DNMR technique (Table 1).

Also in compound **3** two atropisomers with different proportions (57:43) are observed at ambient temperature. Line shape simulation of the two methyl signal as a function of temperature yields the corresponding interconversion barrier (Figure S-6 of the Supporting Information).

To establish unambiguously whether in **3** the anti or the syn is more populated, a NOE experiment was performed (the temperature of −10 °C was used to avoid the effects of saturation transfer). Irradiation of the methyl signal of the syn conformer is expected to enhance two groups of signals, i.e., those of the hydrogens in positions 2,7 of the antraquinone moiety and those of the hydrogens in the position ortho to the methyl group (indicated as 3,3′ in Figure 5). Irradiation of the methyl signal of the anti conformer would enhance the same signals and, in addition, those of the hydrogens in positions 6′ and 6 of the facing ring: in the anti atropisomer, in fact, the methyl in position 2 of one tolyl ring is close to the hydrogen in position 6′ of the other tolyl ring (likewise the methyl in position 2′ is close to the hydrogen in position 6 of the other tolyl). Since irradiation of the major methyl signal displays three significant NOE effects (red middle trace of Figure 5), the corresponding conformation is established to be anti. Again the DFT computations of **3** predict the syn to have an enthalpy lower (by 0.19 kcal mol^{-1}) than that of the anti (Figure S-2 of Supporting Information), but the mentioned correction for the entropy of mixing (RT ln 2) accounts for the greater population observed for the anti form: in this case, in fact, the ΔG^0 of the anti results lower (by 0.19 − 0.41 = −0.22 kcal mol^{-1}) than that of the syn.

In Table 1 are summarized the results obtained for compounds **1**−**3**. The barriers of **2** and **3** are equal within the experimental error (±0.2 kcal mol^{-1}), because in both cases the interconversion involves the passage of the tolyl ring across the C═O moiety. On the other hand the barrier of **1** is significantly higher because the corresponding interconversion requires the passage of the ring across the bulkier CH_2 moiety.

Experimental Section

Materials: 1,8-Di(*o*-tolyl)anthracene-9,10-dione (3). To a solution of 1,8-dichloroanthraquinone (0.277 g, 1.0 mmol, in 10 mL of benzene) were added K_2CO_3 (2 M solution, 5.0 mL), *o*-tolylboronic acid (2.0 mmol, suspension in 2 mL of ethanol), and $Pd(PPh_3)_4$ (0.23 g, 0.2 mmol) at room temperature. The stirred solution was refluxed for 2−3 h, the reaction being monitored by

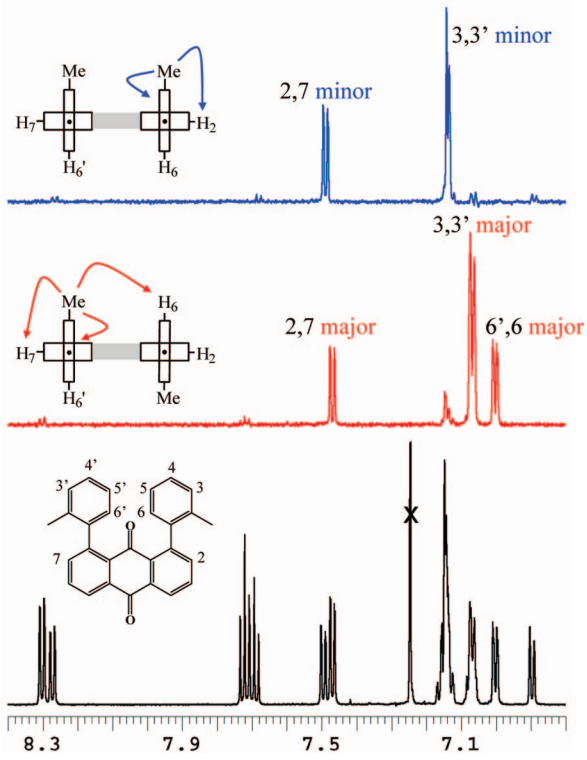

FIGURE 5. Aromatic spectral region (600 MHz at −10 °C in $CDCl_3$) of compound **3** (bottom trace, black). NOE experiments are due to the irradiation of the major methyl signal at 1.98 ppm (middle trace, red) and of the minor methyl signal at 2.08 ppm (top trace, blue).

GC-MS to confirm the first coupling had been achieved. After cooling to room temperature, a second amount of K_2CO_3 (2 M solution, 5.0 mL), *o*-tolylboronic acid (2.0 mmol, suspension in 2 mL of ethanol), and $Pd(PPh_3)_4$ (0.12 g, 0.1 mmol) were added, and the mixture was refluxed again and monitored by GC-MS, until the monochloro intermediate disappeared. To the cooled mixture $CHCl_3$ and H_2O were added and the extracted organic layer was dried (Na_2SO_4) and evaporated. The crude was prepurified by chromatography on silica gel (hexane/Et_2O 10:1) to obtain a mixture containing the target compound contaminated by 1-(*o*-tolyl)anthraquinone and 1-chloro-8-(*o*-tolyl)anthraquinone. Analytically pure **3** was obtained by semipreparative HPLC on a C18 column (10 μm, 250 × 21.2 mm, 24 mL/min, ACN/H_2O; see the Supporting Information for details).

1,8-Di(*o*-tolyl)anthracene-9,10-dione (3). ^{1}H NMR (600 MHz, $CDCl_3$, 25 °C, TMS) δ 1.95 (3.66H, s), 2.05 (2.76H, s), 6.90 (0.88H, d, J = 6.9 Hz), 7.00 (1.23H, m), 7.07 (2.12H, m), 7.15 (4.25H, m), 7.47 (1.14H, dd, J = 7.6, 1.3 Hz), 7.50 (0.86H, dd, J = 7.6, 1.2 Hz), 7.69 (0.86H, t, J = 7.6 Hz), 7.72 (1.14H, t, J = 7.6 Hz), 8.27 (0.86H, dd, J = 7.7, 1.2 Hz), 8.30 (1.14H, dd, J = 7.7, 1.2 Hz); ^{13}C NMR (150.8 MHz, $CDCl_3$, 25 °C, TMS) δ 20.27 (CH_3), 20.31 (CH_3), 125.2 (CH), 125.3 (CH), 126.2 (CH), 126.4 (CH), 127.1 (CH), 127.2 (CH) 127.8 (CH), 128.6 (CH), 129.6 (CH), 129.8 (CH), 131.8 (CH), 132.3 (CH), 133.89 (q), 133.91 (q) 134.2 (q), 134.4 (q), 134.6 (q), 134.8 (q), 137.21 (CH), 137.27 (CH), 140.3 (q), 140.6 (q), 142.48 (q), 141.54 (q), 184.0 (CO), 184.1(CO), 184.6 (CO), 185.5 (CO); HRMS(EI) *m/z* calcd for $C_{28}H_{20}O_2$ 388.14633, found 388.1462.

4,5-Di(*o*-tolyl)anthracen-9(10*H*)-one (1) and 1,8-Di(*o*-tolyl)-anthracen-9(10*H*)-one (2). 1 and **2** were obtained by the Wolf−Kishner reduction[24] of **3**: Hydrazine hydrate (1 mL) and KOH (50 mg, solid) were added to a solution of 1,8-di(*o*-tolyl)anthracene-9,10-dione (100 mg, 0.257 mmol) in a flask equipped with a Dean−Stark apparatus. The stirred solution was refluxed in a oil bath kept at 200 °C for about 3 h, removing the water during the reaction. The brown cooled mixture was extracted with Et_2O, and the extracted organic layer was dried (Na_2SO_4) and evaporated. The crude was prepurified by chromatography on silica gel (hexane/Et_2O 1:1) to obtain a mixture containing the target compounds (in a 1:4 ratio, yield 55%) together with the starting product. Analytically pure samples of **1** and **2** were obtained by semipreparative HPLC on a C18 column (5 μm, 250 × 10 mm, 5 mL/min, ACN/H_2O; see the Supporting Information for details). Crystals of **1** suitable for X-ray analysis were obtained by slow evaporation of a $CHCl_3$ solution. Details of X-ray diffraction data are reported in the Supporting Information.

1,8-Di(*o*-tolyl)anthracen-9(10*H*)-one (2). ^{1}H NMR (600 MHz, $CDCl_3$, 25 °C, TMS) δ 1.94 (3H, s), 2.08 (3H, s), 4.23 (0.5H, d, J = −20.7 Hz), 4.34 (s, 1H), 4.39 (0.5H, d, J = −20.7 Hz), 6.85 (1H, d, J = 7.6 Hz), 6.98−7.18 (9H, m), 7.40−7.50 (4H, m); ^{13}C NMR (150.8 MHz, $CDCl_3$, 25 °C, TMS) δ 20.51 (CH_3), 20.54 (CH_3), 34.3 (CH_2), 34.4 (CH_2), 124.84 (CH), 124.87 (CH), 126.56 (CH), 126.57 (CH), 126.6 (2CH), 126.8 (2CH), 128.0 (CH), 128.7 (CH), 129.2 (CH), 129.6 (CH), 129.8 (CH), 129.9 (CH), 130.2 (CH), 130.8 (CH), 133.3 (q), 134.1 (q), 134.9 (q), 135.2 (q), 139.6 (q), 139.8 (q), 140.9 (q), 141.5 (q), 141.8 (q), 142.2 (q), 185.9 (CO), 187.2 (CO); HRMS(EI) *m/z* calcd for $C_{28}H_{22}O$ 374.16707, found 374.1674

4,5-Di(*o*-tolyl)anthracen-9(10*H*)-one (1). ^{1}H NMR (600 MHz, $CDCl_3$, 25 °C, TMS) δ 1.907 (3H, s), 1.911 (3H, s), 3.14 (0.5H, d, J = −24.0 Hz), 3.34 (s, 1H), 3.51 (0.5H, d, J = −24.0 Hz), 6.94 (2H, m), 7.06−7.18 (6H, m), 7.40 (2H, dt, J = 7.3, 1.7 Hz), 7.52 (2H, t, J = 7.7 Hz), 8.40 (2H, d, J = 8.4 Hz); ^{13}C NMR (150.8 MHz, $CDCl_3$, 25 °C, TMS) δ 19.57 (CH_3), 19.59 (CH_3), 29.6 (CH_2), 29.8 (CH_2), 125.6 (CH), 125.7 (CH), 126.6 (CH), 126.8 (CH), 127.6 (2CH), 128.6 (CH), 128.7 (CH), 129.8 (CH), 129.9 (CH), 132.03 (q), 132.04 (q), 133.4 (2CH), 135.0 (q), 135.2 (q), 138.7 (q), 138.8 (q), 139.04 (q), 139.05 (q), 141.45 (q), 141.47 (q), 184.79 (CO), 184.83 (CO); HRMS(EI) *m/z* calcd for $C_{28}H_{22}O$ 374.16707, found 374.1672.

NMR Spectroscopy. The spectra were recorded at 600 MHz for ^{1}H and 150.8 MHz for ^{13}C. Variable-temperature spectra of **1** were obtained at 400 MHz. The assignments of the ^{1}H and ^{13}C signals were obtained by bidimensional experiments (edited-gsHSQC[25] and gsHMBC[26]). The NOE experiments on **3** were obtained by means of the DPFGSE-NOE[27] sequence. To selectively irradiate the desired signal, a 50 Hz wide shaped pulse was calculated with a refocusing-SNOB shape[28] and a pulse width of 37 ms. Mixing time was set to 1.5 s. Saturation transfer experiments[29] (1D-EXSY) of **1** were obtained by using the same DPFGSE-NOE pulse sequence,[27] raising the mixing time from 25 to 500 ms. Temperature calibrations were performed before the experiments, using a Cu/Ni thermocouple immersed in a dummy sample tube filled with 1,1,2,2-tetrachloroethane, and under conditions as nearly identical as possible. The uncertainty in the temperatures was estimated from the calibration curve to be ±1

(23) Lomas, J. S.; Cordier, C. *J. Phys. Org. Chem.* **2003**, *16*, 361–368. Mazzanti, A.; Lunazzi, L.; Minzoni, M.; Anderson, J. E. *J. Org. Chem.* **2006**, *71*, 5474–5481. Lunazzi, L.; Mazzanti, A.; Minzoni, M. *J. Org. Chem.* **2007**, *72*, 2501–2507. Lunazzi, L.; Mazzanti, A.; Rafi, S.; Rao, H. S. P. *J. Org. Chem.* **2008**, *73*, 678–688.

(24) Kishner, N. J. *Russ. Phys. Chem. Soc.* **1911**, *43*, 582. Wolff, L. *Ann.* **1912**, *394*, 86. Todd, D. *Org. React.* **1948**, *4*, 378.

(25) Bradley, S. A.; Krishnamurthy, K. *Magn. Reson. Chem.* **2005**, *43*, 117. Kupče, E.; Freeman, R. *J. Magn. Reson. A* **1996**, *118*, 299–303. Willker, W.; Leibfritz, D.; Kerssebaum, R.; Bermel, W. *Magn. Reson. Chem.* **1993**, *31*, 287–292.

(26) Hurd, R. E.; John, B. K. *J. Magn. Reson.* **1991**, *91*, 648.

(27) (a) Stott, K.; Stonehouse, J.; Keeler, J.; Hwand, T.-L.; Shaka, A. J. *J. Am. Chem. Soc.* **1995**, *117*, 4199. (b) Stott, K.; Keeler, J.; Van, Q. N.; Shaka, A. J. *J. Magn. Reson.* **1997**, *125*, 302. (c) Van, Q. N.; Smith, E. M.; Shaka, A. J. *J. Magn. Reson.* **1999**, *141*, 191. (d) See also: Claridge, T. D. W. *High Resolution NMR Techniques in Organic Chemistry*; Pergamon: Amsterdam, The Netherlands, 1999.

(28) Kupče, E.; Boyd, J.; Campbell, I. D. *J. Magn. Reson. Ser. B* **1995**, *106*, 300.

(29) Forsén, S.; Hoffmann, R. A. *Acta Chem. Scand.* **1963**, *17*, 1787–1788.

°C. The line shape simulations were performed by means of a PC version of the QCPE program DNMR 6 no. 633, Indiana University, Bloomington, IN.

Calculations. Geometry optimizations were carried out at the B3LYP/6-31G(d) level by means of the Gaussian 03 series of programs[30] (see the Supporting Information). In the case of **1**-*syn*, geometry optimization was also carried out at the B3LYP/6-31++G(d,p), PBE1PBE/6-31+G(d,p), and HF/6-31+G(d,p) level. The standard Berny algorithm in redundant internal coordinates and default criteria of convergence were employed in all calculations. Reported energies include unscaled ZPE and thermal correction to enthalpy. Harmonic vibrational frequencies were calculated for all the stationary points. For each optimized ground state the frequency analysis showed the absence of imaginary frequencies. Chemical shift and *J*-coupling calculations were obtained at the B3LYP/6-31+G(d,p) level by using the option that includes the Fermi contact contribution.

Acknowledgment. L.L. and A.M. received financial support from the University of Bologna (RFO) and from MUR-COFIN 2005, Rome (national project "Stereoselection in Organic Synthesis").

Supporting Information Available: DFT optimized geometry of **2** and **3**, high-resolution ^{1}H spectrum of **2**, ^{13}C spectra of **1** in chiral medium, VT spectra and simulation of **1**−**3**, X-ray diffraction data of **1**, 1D-EXSY kinetic data, copy of ^{1}H, ^{13}C NMR spectra, and HPLC traces of **1**−**3**, and computational data of **1**−**3**. This material is available free of charge via the Internet at http://pubs.acs.org.

JO800677N

(30) Frisch, M. J.; Trucks, G. W.; Schlegel, H. B.; Scuseria, G. E.; Robb, M. A.; Cheeseman, J. R.; Montgomery, J. A., Jr.; Vreven, T.; Kudin, K. N.; Burant, J. C.; Millam, J. M.; Iyengar, S. S.; Tomasi, J.; Barone, V.; Mennucci, B.; Cossi, M.; Scalmani, G.; Rega, N.; Petersson, G. A.; Nakatsuji, H.; Hada, M.; Ehara, M.; Toyota, K.; Fukuda, R.; Hasegawa, J.; Ishida, M.; Nakajima, T.; Honda, Y.; Kitao, O.; Nakai, H.; Klene, M.; Li, X.; Knox, J. E.; Hratchian, H. P.; Cross, J. B.; Bakken, V.; Adamo, C.; Jaramillo, J.; Gomperts, R.; Stratmann, R. E.; Yazyev, O.; Austin, A. J.; Cammi, R.; Pomelli, C.; Ochterski, J. W.; Ayala, P. Y.; Morokuma, K.; Voth, G. A.; Salvador, P.; Dannenberg, J. J.; Zakrzewski, V. G.; Dapprich, S.; Daniels, A. D.; Strain, M. C.; Farkas, O.; Malick, D. K.; Rabuck, A. D.; Raghavachari, K.; Foresman, J. B.; Ortiz, J. V.; Cui, Q.; Baboul, A. G.; Clifford, S.; Cioslowski, J.; Stefanov, B. B.; Liu, G.; Liashenko, A.; Piskorz, P.; Komaromi, I.; Martin, R. L.; Fox, D. J.; Keith, T.; Al-Laham, M. A.; Peng, C. Y.; Nanayakkara, A.; Challacombe, M.; Gill, P. M. W.; Johnson, B.; Chen, W.; Wong, M. W.; Gonzalez, C.; Pople, J. A. *Gaussian 03*, Revision D.01; Gaussian, Inc.: Wallingford CT, 2004.